

Multielectron photoionization to the $3p^4 4p$ configuration of Ar^+ : Experiment and theory

W. T. Silfvast, D. Y. Al-Salameh, and O. R. Wood II

AT&T Bell Laboratories, Crawfords Corner Road, Holmdel, New Jersey 07733-1988

(Received 18 July 1986)

Short-pulse (100-psec) soft-x-ray excitation from a laser-produced plasma and fast optical detection have been used to study multielectron photoionization from the $3p^6$ neutral ground state to the ten terms of the $3p^4 4p$ configuration of Ar^+ . Good agreement between measured populations and those obtained from an excitation model based on energy-dependent cross sections calculated with a relativistic Hartree-Fock atomic physics code using configuration interaction techniques was obtained.

A 100-psec duration soft-x-ray pulse from a laser-produced plasma combined with a subnanosecond optical detection system has been used to study electron correlations in Ar by observing multielectron photoionization from the $3p^6$ ground state of neutral Ar to the $3p^4 4p$ configuration of Ar^+ . Measured population densities of the ten LS terms of this configuration produced by direct two-electron photoionization are in reasonably good agreement with those predicted by an excitation model based upon calculated photoionization cross sections to these ten terms and a measured soft-x-ray flux equivalent to an approximately 23-eV blackbody. The energy-dependent cross sections were computed with an atomic physics code using configuration interaction (CI) techniques. The sum of two of the calculated partial cross sections, with a peak value of 0.06 Mb at 40 eV (310 Å), agrees within 30% over a wide range of energies with a cross section for those terms deduced from satellite intensities measured with photoelectron spectroscopy.

When atoms are photoionized, observation of secondary processes involving excitation of more than one electron can be used to interpret the nature of the coupling or correlation between the electrons of the atom, not only in their initial and final states but also in the dynamics of the readjustment during the electron departure. Secondary photoionization can occur as a result of three processes:¹ The first is the "shake" type of process² dominant at higher energies. The second is the result of electron correlations in the initial and final ionic states giving rise to configuration interactions. The third is interchannel coupling¹ which results from interactions between various final states by means of the continuum. The present investigation involves studies of the second process, the effect of electron correlations.

Evidence of secondary processes were first observed in absorption spectroscopy³ but were often obscured by the primary one-electron processes. In many atoms secondary processes have been studied with photoelectron spectroscopy through the presence of satellite lines⁴ in the photoelectron spectrum. However, in cases where there are a large number of closely spaced excited states, identification is not possible either because of low resolution or because of the presence of other background emissions. Because the experimental technique described in this Rapid Communication monitors the emission from the various

multielectron excited states immediately after the excitation terminates, before cascade or electron collisional relaxation can occur, it can be used to study multielectron excitations that are not well suited to either absorption or photoelectron spectroscopy.

The experimental arrangement used to study multielectron photoionization of Ar is similar to that used recently⁵ to study autoionizing levels in Cd^+ . A 100-psec duration, 25-mJ pulse from a neodymium-doped yttrium aluminum garnet laser is focused onto a Ta target in a cell containing flowing Ar gas at 10-Torr pressure resulting in an intense pulse of soft x rays from the target surface and multielectron photoionization of the argon gas. The relative intensities of the near ultraviolet, blue and green emission from the 21 fine-structure states of the $3p^4 4p$ configuration of Ar^+ were measured immediately after the termination of the soft-x-ray pulse with a detection system that included a lens arrangement to permit observations at various distances above the soft-x-ray source, a spectrometer capable of 0.2-Å resolution, a 150-psec rise time microchannel-plate photomultiplier, and a 500-MHz oscilloscope. The magnitude of the population inversion created between one of these states, the $3p^4(^3P)4p^2P_{3/2}$ state of Ar^+ , and the lower-lying $3p^4(^3P)4s^2P_{1/2}$ state was determined (1) by passing a 2-mW cw probe beam from an argon-ion laser operating on that transition at 4765 Å through the argon gas 0.5 cm above the soft-x-ray source and (2) by measuring the ratio of the double- to single-pass emission at 4765 Å in the presence and in the absence of a mirror behind the photoionized region of argon. Both techniques indicated a gain-length product of approximately 0.6, which corresponds to a $3p^4(^3P)4p^2P_{3/2}$ state population of $1.3 \times 10^{11} \text{ cm}^{-3}$ assuming that the linewidth is predominantly Doppler broadened and that photoionization occurs predominantly to the $3p^4(^3P)4p^2P_{3/2}$ upper state [photoelectron spectra of argon⁶ in the energy region of the lower-lying $3p^4(^3P)4s^2P_{1/2}$ state shows no significant excitation]. Population densities of the remaining 20 fine-structure states were then obtained from the relative intensity data (after correcting for the wavelength dependence of the detector and spectrometer grating) using known transition probabilities⁷ for the various emission lines. The populations of the 21 states were then combined according to their respective LS terms to provide a comparison with theory.

The measured population densities of the ten LS terms of the $3p^4 4p$ configuration of Ar^+ are shown in Fig. 1 (solid bars) at their respective energy locations with respect to the Ar neutral ground state. For comparison, population densities determined from calculated values for the cross sections and an estimated pumping flux (discussed later) are also shown in Fig. 1 (open vertical bars). The $3p^4(^3P)4p^2P^o$ and $3p^4(^1D)4p^2P^o$ terms are the most highly populated. This is consistent with the earlier observations of strong photoelectron satellites⁶ in the energy regions of the states belonging to those terms.

In order to obtain a theoretical basis for the photoionization measurements, an atomic physics code using configuration interaction techniques⁸ in which each continuum region was treated as a pseudodiscrete state, was used to calculate the individual photoionization cross sections to the ten LS terms of the $3p^4 4p$ configuration of Ar^+ over an energy range from 36 to 52 eV (345–240 Å). For each configuration, radial integrals were calculated using the relativistic Hartree-Fock method. This was followed by the calculation of the angular coefficients of the various CI radial and electric dipole integrals. After constructing all possible sets of quantum numbers using the LS coupling scheme, the above parameters were used to construct the CI matrix and to calculate energy level positions and transition probabilities. Contribution of the initial-state CI (ISCI) to the cross section for photoionizing the $3p^6$ ground configuration to the $3p^4 4p$ ion configuration (which is proportional to the transition probability of $3p^6-3p^4 4p \epsilon s, \epsilon d$ continua) was calculated via interaction of $3p^6$ with three configurations, namely, $3p^5 4p$, $3p^4 4p 4f$, and $3p^4 4p^2$ (the three configurations have nonzero dipole

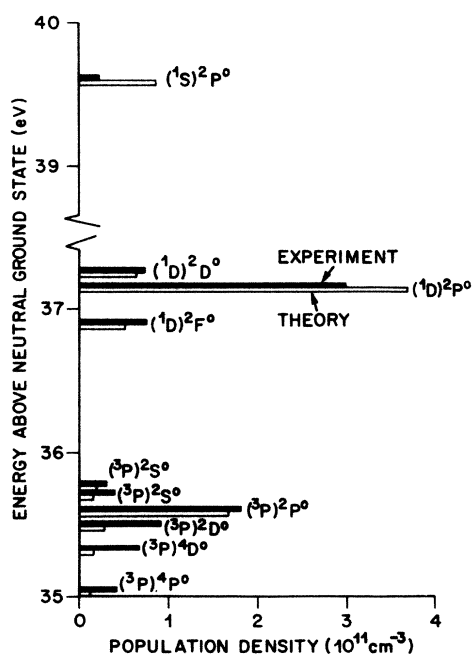


FIG. 1. Bar graph of the population densities of the $3p^4 4p$ Ar^+ LS terms energetically located with respect to the neutral $3p^6$ Ar ground state. Experimental values are shown as solid bars and theoretical values are shown as open bars for each term.

matrix elements to the continuum). The final ionic-state configuration interaction (FISCI) contribution was obtained by calculating the transition probability of $3p^6-3p^5 4s$, $3d$ (electric dipole allowed) and the CI of $3p^5 4s$, $3d$ with $3p^4 4p \epsilon s, \epsilon d$ continua. In both cases the interaction of $3p^4 4p ns, nd$ with $4p^4 4p \epsilon s, \epsilon d$ and the interactions among continua was taken into account. All calculations of dipole matrix elements were carried out using the length formulation. The contributions of final-state-continuum s electrons were found to be minimal when compared to the contributions of continuum d electrons.

The calculated partial cross sections which include both ISCI and FISCI contributions together with the total cross section (the sum of the ten individual cross sections) are shown in Fig. 2(a). In most cases, ISCI is the dominant process. The $3p^5 4p^1 S_0$ state was found to make the dom-

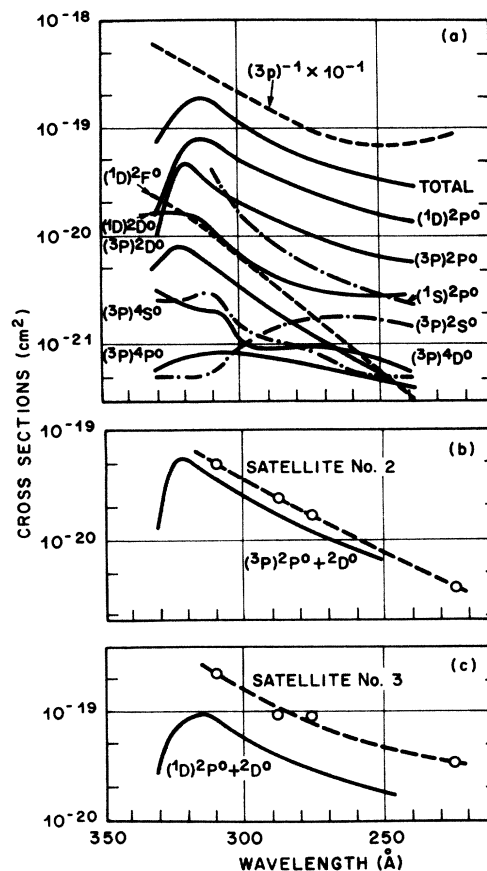


FIG. 2. Photoionization cross sections from the $3p^6$ ground state of Ar to the $3p^4 4p$ configuration of Ar^+ . (a) Individual cross sections to the ten LS terms using an atomic-physics code with configuration interactions. Also shown are the total combined cross section of the ten terms, and the cross section (at a reduced value) for removing one $3p$ electron to produce the Ar^+ ground state (upper dashed curve). (b) Combined partial theoretical cross sections for the $3p^4(^3P)4p(^2P^o+2D^o)$ terms compared to cross sections for satellite production using photoelectron spectroscopy at the same energy location as those terms. (c) Combined partial theoretical cross sections for the $3p^4(^1D)4p(^2P^o+2D^o)$ terms compared to satellite production at the same energy.

inant contribution to ISCI since it is the most strongly mixed with $3p^6 1S_0$. Strong dipole coupling of this state to the $3p^4 4p \epsilon d^1 P_1$ continuum states [with both (1D) and (3P) cores] leads to the dominant production of both (1D) $^2P^\circ$ and (3P) $^2P^\circ$ terms in the $Ar^+ 3p^4 4p$ configuration. This is confirmed by the experimental population density measurements shown in Fig. 1. The weak production of quartet terms, also shown in Fig. 1, results from their predominant origination from quintet and triplet continuum states which are only weakly coupled to the $3p^5 4p^1 S_0$ state. There are a few exceptions to the dominance of ISCI: The FISCI contribution to the cross section for the $3p^4(^1D)4p^2 F^\circ$ term is more than an order of magnitude greater than the ISCI contribution. This result is supported by the good agreement between the experimental and theoretical population densities for that term shown in Fig. 1. The cross section for the $3p^4(^3P)4p^2 D^\circ$ state also has a slightly higher contribution from FISCI and in the cross section for the $3p^4(^3P)4p^4 S^\circ$ term the contributions are comparable. For comparison, the measured cross section for the removal of a single $3p$ electron, $(3p)^{-1}$ (which results in the $3p^5$ ground configuration of Ar^+), is also shown in Fig. 2(a) (on a reduced scale). The similar energy dependences of most of the partial cross sections of $3p^4 4p$ with this cross section suggests that most are affected by correlation processes occurring in the $3p$ subshell.

In a recent photoelectron spectrum of argon⁶ a satellite at 35.6 eV (No. 2) was tentatively assigned to the $3p^4(^3P)4p^2 D^\circ$ or $3p^4(^3P)4p^2 P^\circ$ term of Ar^+ because the energies of the states belonging to those terms fall within the satellite envelope. From the total cross section for the sum of the four satellites (Nos. 1, 2, 3, and 4') and the partial intensities of the individual satellite components given in that work, and assuming that the widths of the satellites were the same at all energies, the cross section for the production of that satellite shown in Fig. 2(b), was deduced. For comparison, calculated values for the sum of the cross sections for the $3p^4(^3P)4p^2 D^\circ$ and $3p^4(^3P)4p^2 P^\circ$ terms are also shown in Fig. 2(b). The agreement between experimental and theoretical values is within 30% over most of the energy range. This suggests that the $3p^4(^3P)4p^2 P^\circ$ term is primarily responsible for that satellite and that ISCI dominates the photoionization process to this term.

The cross section for a satellite at 37.2 eV (No. 3), tentatively assigned⁶ to either the $3p^4(^1D)3d^2 D^\circ$, $3p^4(^1D)4p^2 D^\circ$, or $3p^4(^1D)4p^2 P^\circ$ of Ar^+ , is shown in Fig. 2(c). For comparison, calculated values for the sum of the cross sections for two of those terms [from Fig. 2(a)], the $3p^4(^1D)4p^2 P^\circ$ and $3p^4(^1D)4p^2 D^\circ$ terms, is also shown in Fig. 2(c). Even though this cross section is supported by the good agreement between the measured and calculated population densities shown in Fig. 1 for these terms it is only 40% of the measured satellite cross section. There are two possible explanations for this difference: Other secondary processes, in addition to ISCI and FISCI, could contribute to the cross section or the $3p^4(^1D)3d^2 D^\circ$ term is the dominant component. The second explanation is more likely since that assignment is consistent with the mea-

sured asymmetry parameter⁶ for satellite No. 3 which suggests that it does not result from a $3p^4 4p^2 P^\circ$ term.

The close agreement between the calculated and measured cross sections shown in Fig. 2(b) provides confidence in the calculated cross sections, particularly for the $3p^4(^3P)4p^2 P^\circ$ term. The accuracy of the calculated cross sections for the other nine terms can be estimated by comparing populations based on an excitation model (discussed later) with accurate population measurements which can only be made by using both a fast excitation pulse and a fast measurement system to determine the population in a time short compared to the decay time of the states of those terms (radiative decay times of those states are of the order of 5–10 nsec and collisional decay times are no faster than a nsec for the electron densities of this experiment). An excitation model was developed based on the theoretical cross sections presented in Fig. 2(a) and on an estimate of the magnitude of the soft-x-ray flux. Based on earlier work, the soft-x-ray flux was assumed to originate from a circular area of 0.0125-cm radius on the target surface and be confined to a solid angle of approximately $\pi/2$ in the argon gas. The temperature of the source (assumed to have a blackbody distribution) was determined by integrating the flux over the experimentally determined cross section of Fig. 2(b), and adjusting the temperature to produce agreement with the sum of the measured $3p^4(^3P)4p^2 P^\circ$ and $^2 D^\circ$ term population densities shown in Fig. 1. The resulting temperature, 23 eV, was then used in combination with the theoretical cross sections of Fig. 2(a) to calculate the population densities of all ten LS terms of the $3p^4 4p$ configuration (open vertical bars of Fig. 1).

The agreement between measured and calculated population densities shown in Fig. 1 is quite good for all but the lowest and highest terms. The slightly poorer agreement of these terms could be due to missing configurations in the calculations, collisional transfer of energy from or to nearby states of other configurations during the measurement time, shake processes, interchannel coupling, or a nonblackbody distribution of the pumping flux. Since all of the relevant configurations are thought to have been used in the code and since known mixing cross sections⁹ suggest that collisions do not have a major effect for the plasma conditions of this experiment, and shake processes are not generally applicable near threshold,² the latter two explanations seem to be most likely. Interchannel coupling effects cannot be distinguished in the present experiment. Recently published spectral distributions of laser-produced plasma emission in the relevant spectral range at intensities used in the present experiment¹⁰ clearly show a deviation from a blackbody distribution and could account for the differences shown in Fig. 1.

The authors wish to acknowledge helpful discussions with R. D. Cowan, R. P. Madden, T. B. Lucatorto, and S. E. Harris and the technical assistance of T. E. Harvey in performing the experimental measurements and reducing the cross-section data.

- ¹U. Becker, R. Holzel, H. G. Kerkhoff, B. Langer, D. Szostak, and R. Wehlitz, *Phys. Rev. Lett.* **56**, 1120 (1986).
- ²T. D. Thomas, *Phys. Rev. Lett.* **52**, 417 (1984).
- ³R. P. Madden, D. L. Ederer, and K. Codling, *Phys. Rev.* **177**, 136 (1969).
- ⁴K. G. Dyall and F. P. Larkins, *J. Phys. B* **15**, 203 (1982); **15**, 219 (1982).
- ⁵O. R. Wood II, W. T. Silfvast, J. J. Macklin, and P. J. Maloney, *Opt. Lett.* **11**, 198 (1986).
- ⁶M. Y. Adam, P. Morin, and G. Wendin, *Phys. Rev. A* **31**, 1426 (1985).
- ⁷W. L. Wiese, M. W. Smith, and B. M. Miles, *Atomic Transition Probabilities* (U.S. GPO, Washington, DC, 1969), Vol. II.
- ⁸R. D. Cowan, *Theory of Atomic Structure and Spectra* (University of California Press, Berkeley, 1981), Secs. 8-1 and 16-1.
- ⁹T. Sakurai, *J. Appl. Phys.* **45**, 2666 (1974), and references therein.
- ¹⁰J. M. Bridges, C. L. Cromer, and T. J. McIlrath, *Appl. Opt.* **25**, 2208 (1986).